Cross-platform validation of neurotransmitter release impairments in schizophrenia patient-derived *NRXN1*-mutant neurons

ChangHui Pak[a,b,c,1,2], Tamas Danko[a,d,1], Vincent R. Mirabella[e,f], Jinzhao Wang[a,d], Yingfei Liu[d], Madhuri Vangipuram[d], Sarah Grieder[d], Xianglong Zhang[g], Thomas Ward[g], Yu-Wen Alvin Huang[a,b,3], Kang Jin[h,i], Philip Dexheimer[h,i], Eric Bardes[h,i], Alexis Mitelpunkt[h,i,j], Junyi Ma[k], Michael McLachlan[k], Jennifer C. Moore[l,m], Pingping Qu[g], Carolin Purmann[g], Jeffrey L. Dage[n], Bradley J. Swanson[k,4], Alexander E. Urban[g,o], Bruce J. Aronow[h,i], Zhiping P. Pang[e,f], Douglas F. Levinson[g], Marius Wernig[d,p], and Thomas C. Südhof[a,b,2]

[a]Department of Molecular & Cellular Physiology, Stanford University School of Medicine, Stanford, CA 94305; [b]Howard Hughes Medical Institute, Stanford University School of Medicine, Stanford, CA 94305; [c]Department of Biochemistry & Molecular Biology, University of Massachusetts, Amherst, MA 01003; [d]Institute for Stem Cell Biology and Regenerative Medicine, Stanford University School of Medicine, Stanford, CA 94305; [e]Child Health Institute of New Jersey, Rutgers Robert Wood Johnson Medical School, New Brunswick, NJ 08901; [f]Department of Neuroscience and Cell Biology, Rutgers Robert Wood Johnson Medical School, New Brunswick, NJ 08901; [g]Department of Psychiatry & Behavioral Sciences, Stanford University School of Medicine, Stanford, CA 94305; [h]Department of Biomedical Informatics, University of Cincinnati, Cincinnati Children's Hospital Medical Center, Cincinnati, OH 45229; [i]Department of Pediatrics, University of Cincinnati, Cincinnati Children's Hospital Medical Center, Cincinnati, OH 45229; [j]Sackler Faculty of Medicine, Tel Aviv University, Tel Aviv, Israel 6997801; [k]Fujifilm Cellular Dynamics, Inc., Madison, WI 53711; [l]Rutgers University Cell and DNA Repository Infinite Biologics, National Institute of Mental Health Repository and Genomics Resource, Rutgers University, Piscataway, NJ 08854; [m]Department of Genetics, Rutgers University, Piscataway, NJ 08854; [n]Eli Lilly and Company, Indianapolis, IN 46285; [o]Department of Genetics, Stanford University School of Medicine, Stanford, CA 94305; and [p]Department of Pathology, Stanford University School of Medicine, Stanford, CA 94305

Contributed by Thomas C. Südhof, April 15, 2021 (sent for review December 13, 2020; reviewed by Jaewon Ko, Susanne Schoch, Hongjun Song, and Matthew State)

Heterozygous *NRXN1* deletions constitute the most prevalent currently known single-gene mutation associated with schizophrenia, and additionally predispose to multiple other neurodevelopmental disorders. Engineered heterozygous *NRXN1* deletions impaired neurotransmitter release in human neurons, suggesting a synaptic pathophysiological mechanism. Utilizing this observation for drug discovery, however, requires confidence in its robustness and validity. Here, we describe a multicenter effort to test the generality of this pivotal observation, using independent analyses at two laboratories of patient-derived and newly engineered human neurons with heterozygous *NRXN1* deletions. Using neurons transdifferentiated from induced pluripotent stem cells that were derived from schizophrenia patients carrying heterozygous *NRXN1* deletions, we observed the same synaptic impairment as in engineered *NRXN1*-deficient neurons. This impairment manifested as a large decrease in spontaneous synaptic events, in evoked synaptic responses, and in synaptic paired-pulse depression. *Nrxn1*-deficient mouse neurons generated from embryonic stem cells by the same method as human neurons did not exhibit impaired neurotransmitter release, suggesting a human-specific phenotype. Human *NRXN1* deletions produced a reproducible increase in the levels of CASK, an intracellular *NRXN1*-binding protein, and were associated with characteristic gene-expression changes. Thus, heterozygous *NRXN1* deletions robustly impair synaptic function in human neurons regardless of genetic background, enabling future drug discovery efforts.

neurexin | synapse formation | schizophrenia | NMDA receptor | synaptic transmission

Significance

Heterozygous *NRXN1* deletions predispose to schizophrenia and other neurodevelopmental disorders. Engineered heterozygous *NRXN1* deletions impair neurotransmitter release in human neurons, suggesting a synaptic pathophysiological mechanism. In a multicenter effort to test the generality and robustness of this pivotal observation, we used, at two laboratories, independent analyses of patient-derived and newly engineered human neurons with heterozygous *NRXN1* deletions. Schizophrenia patient-derived neurons with *NRXN1* deletions exhibited the same major decrease in neurotransmitter release and an increase in CASK protein as engineered human neurons with *NRXN1* deletions. Strikingly, engineered mouse *Nrxn1*-deficient neurons derived by the same method displayed no such phenotype, suggesting a human-specific role for *NRXN1*. Thus, heterozygous *NRXN1* deletions robustly impair synaptic function in human neurons, enabling future drug discovery efforts.

Schizophrenia is a devastating brain disorder that affects millions of people worldwide and exhibits a strong genetic component. In a key discovery, deletions or duplications of larger stretches of chromosomal DNA that lead to copy number variations (CNVs) were identified two decades ago (1, 2). CNVs occur unexpectedly frequently, are often de novo, and usually affect multiple genes depending on the size of the deleted or duplicated stretch of DNA. Strikingly, the biggest genetic risk for schizophrenia was identified in three unrelated CNVs: a duplication of region 16p11.2 and deletions of 22q11.2 and of 2p16.3 (3–9). Of these CNVs, 16p11.2 and 22q11.2 CNVs affect more than 20 genes,

Author contributions: C.P., T.D., V.R.M., J.W., Y.L., M.V., S.G., X.Z., T.W., Y.-W.A.H., K.J., P.D., E.B., A.M., J.M., M.M., J.C.M., P.Q., C.P., J.L.D., B.J.S., A.E.U., B.J.A., Z.P.P., D.F.L., M.W., and T.C.S. designed research; C.P., T.D., V.R.M., J.W., Y.L., M.V., S.G., X.Z., T.W., Y.-W.A.H., K.J., P.D., E.B., A.M., J.M., M.M., J.C.M., P.Q., C.P., J.L.D., and B.J.S. performed research; C.P. and M.M. contributed new reagents/analytic tools; C.P., T.D., V.R.M., J.W., Y.L., M.V., S.G., X.Z., T.W., Y.-W.A.H., K.J., P.D., E.B., A.M., J.M., M.M., J.C.M., P.Q., C.P., J.L.D., B.J.S., A.E.U., B.J.A., Z.P.P., D.F.L., M.W., and T.C.S. analyzed data; C.P., T.D., V.R.M., J.W., Y.L., M.V., S.G., X.Z., T.W., Y.-W.A.H., K.J., P.D., E.B., A.M., J.M., M.M., J.C.M., P.Q., C.P., J.L.D., B.J.S., A.E.U., B.J.A., Z.P.P., D.F.L., M.W., and T.C.S. wrote the paper; and D.F.L. administered the entire program.

Reviewers: J.K., Daegu Gyeongbuk Institute of Science and Technology; S.S., University of Bonn; H.S., University of Pennsylvania; and M.S., University of California San Francisco.

Competing interest statement: This was an NIH-mandated academia–industry collaboration. The following authors were employees of companies with an active interest in the research: J.M. and M.M. of Fujifilm Cellular Dynamics and J.L.D. of Eli Lilly and Company.

[1]C.P. and T.D. contributed equally to this work.

[2]To whom correspondence may be addressed. Email: cpak@umass.edu or tcs1@stanford.edu.

[3]Present address: Department of Molecular Biology, Cell Biology, and Biochemistry, Brown University, Providence, RI 02912.

[4]Present address: Promega Inc., Madison, WI 53711.

This article contains supporting information online at https://www.pnas.org/lookup/suppl/doi:10.1073/pnas.2025598118/-/DCSupplemental.

Published May 25, 2021.

whereas 2p16.3 CNVs impact only one or more exons of a single gene, *NRXN1*, which encodes the presynaptic cell-adhesion molecule neurexin-1 (4, 7, 9–12). *NRXN1* CNVs confer an approximately 10-fold increase in risk of schizophrenia, and additionally strongly predispose to other neuropsychiatric disorders, especially autism and Tourette syndrome (13, 14). Moreover, genome-wide association studies using DNA microarrays identified common changes in many other genes that predispose to schizophrenia with smaller effect sizes (15–21). Viewed together, these studies indicate that variations in a large number of genes are linked to schizophrenia. Among these genetic variations, heterozygous exonic CNVs of *NRXN1* are rare events, but nevertheless constitute the most prevalent high-risk single-gene association at present.

Neurexins are central regulators of neural circuits that control diverse synapse properties, such as the presynaptic release probability, the postsynaptic receptor composition, and synaptic plasticity (22–28). To test whether heterozygous *NRXN1* mutations might cause functional impairments in human neurons, we previously generated conditionally mutant human embryonic stem (ES) cells that enabled induction of heterozygous *NRXN1* deletions using Cre-recombinase (29). We then analyzed the effects of the deletion on the properties of neurons induced from the conditionally mutant ES cells using forced expression of Ngn2, a method that generates a relatively homogeneous population of excitatory neurons that are also referred to as induced neuronal (iN) cells (30). These experiments thus examined isogenic neurons without or with a heterozygous *NRXN1* loss-of-function mutation that mimicked the schizophrenia-associated 2p16.3 CNVs, enabling precise control of the genetic background. The heterozygous *NRXN1* deletion produced a robust but discrete impairment in neurotransmitter release without major changes in neuronal development or morphology (29). These results were exciting because they suggested that a discrete impairment in neurotransmitter release could underlie the predisposition to schizophrenia conferred by the 2p16.3 CNV, but these experiments did not reveal whether the *NRXN1* mutation induces the same synaptic impairment in schizophrenia patients (31).

The present project was initiated to achieve multiple overlapping aims emerging from the initial study on human *NRXN1* mutations (29). First, we aimed to validate or refute the results obtained with neurons generated from engineered conditionally mutant ES cells with neurons generated from patient-derived induced pluripotent stem (iPS) cells containing *NRXN1* mutations (Fig. 1*A*). This goal was pursued in order to gain confidence in the disease-relevance of the observed phenotypes. Second, we wanted to test whether the observed phenotype is independent of the laboratory of analysis (i.e., whether it is sufficiently robust to be replicated at multiple sites) (Fig. 1*A*). This goal was motivated by the observation of limited reproducibility in some studies of the phenotypes of patient-derived neurons. We hypothesized that this lack of reproducibility is due to variations in experimental conditions rather than an experimental failure, and designed our studies to demonstrate robustness of the findings through replication. Third, we aimed to generate reagents that could be broadly used by the scientific community for investigating the cellular basis of neuropsychiatric disorders (32). This goal was prompted by the challenges posed by the finding that many different genes appear to be linked to schizophrenia. Fourth, we aimed to definitively establish or exclude the possibility that human neurons are uniquely sensitive to a heterozygous loss of *NRXN1* compared with mouse neurons (Fig. 1*B*). The goal here was to test whether at least as regards to *NRXN1*, mouse and human neurons exhibit fundamental differences. Fifth and finally, we hoped to gain further insights into the mechanisms by which *NRXN1* mutations predispose to schizophrenia, an obviously needed objective given our lack of understanding of this severe disorder. As described in detail below, our data provide advances toward meeting these goals, establishing unequivocally that heterozygous *NRXN1* deletions in human but not in mouse neurons cause a robust impairment in neurotransmitter release that is replicable in multiple laboratories.

Results

Cohort of Cases and Controls. Peripheral blood mononuclear cell (PBMC) specimens and genomic DNA were obtained from the National Institute of Mental Health Repository and Genomics Resource, donated by schizophrenia patients carrying heterozygous *NRXN1* exonic deletions and control individuals who were participants in the Molecular Genetics of Schizophrenia (MGS2) European-ancestry cohort (33). The controls met criteria that predicted low genetic risk for schizophrenia. Cases and controls were aged 35 to 51 y at collection (*Materials and Methods* and *SI Appendix*, Table S1) (for the availability of nonidentified clinical information and of biomaterials, see https://www.nimhgenetics.org/). Controls were selected based on low schizophrenia polygenic risk scores and educational/occupational characteristics suggesting absence of either superior or deficient cognitive function. iPS cell lines were generated from PBMCs by the Rutgers University Cell and DNA Repository (RUCDR) via integration-free Sendai virus reprogramming. Three subclones were generated from each line for analysis (Fig. 1). Reprogramming included extensive quality-control measures to verify normal karyotypes, morphology, and pluripotency of iPS cells, which were also tested pre- and post-freezing for mycoplasma, and whole-genome sequencing (WGS) validated the presence of an exonic *NRXN1* deletion in patients but not in controls (*SI Appendix*, Fig. S1). No patient or control carried other exonic CNVs known to be associated with schizophrenia or contained nonsynonymous single-nucleotide variants, except for a variant in N1884 (chr2:50724817G > A [hg19]; chr2:50497679G > A [hg38]), which is predicted to be benign.

Of the five lines with *NRXN1* deletions (referred to as $NRXN1^{del}$) and the six control lines available, we selected three pairs of $NRXN1^{del}$ cases and controls based on similarity in gender and age at donation (*SI Appendix*, Table S1). Two selected lines had deletions affecting only NRXN1α, while the third line had a deletion ablating both NRXN1α and NRXN1β (*SI Appendix*, Fig. S1*A*). All subsequent differentiations, functional assays, and data analyses were performed using this pairing system, such that each patient-derived human iPS cell line was consistently paired with its own human control iPS cell line to minimize experimental and line-to-line variability. This approach does not imply genetic similarity between cases and controls as the pairing is by necessity random. Frozen vials of iPS cells were shipped for cell line expansion, banking, and iN cell transdifferentiation to generate human neurons at two sites, Stanford University and FUJIFILM Cellular Dynamics Inc. (FCDI) (Fig. 1). The neurons generated at Stanford University were then also analyzed at Stanford, whereas the neurons generated at FCDI were shipped for analysis to Rutgers University.

Single-Laboratory vs. Industry-Scale Methods of Ngn2-Induced Transdifferentiation of iPS Cells into Neurons. Forced expression of Ngn2 rapidly converts human ES or iPS cells into excitatory neurons (29, 30, 34). These human neurons, also referred to as iN cells, are composed of excitatory, relatively homogeneous neurons resembling cortical layer 2/3 pyramidal neurons (30). Since production of Ngn2-induced human neurons is robust and scalable, we decided to further optimize it with two specific goals in mind: 1) to generate human neurons by transdifferentiation of iPS cells that are grown on feeder cell layers, which was necessary to minimize karyotypic abnormalities; and 2) to manufacture human neurons at an industry scale, thus enabling distribution of human neurons to multiple sites for downstream functional studies.

Guided by our published protocols (35) (*Materials and Methods*), we modified the iPS cell dissociation step to efficiently remove mouse feeder cells from human iPS cell colonies. We also improved the initial induction step to provide the optimal medium combination for cell survival and TetO-inducible Ngn2 expression

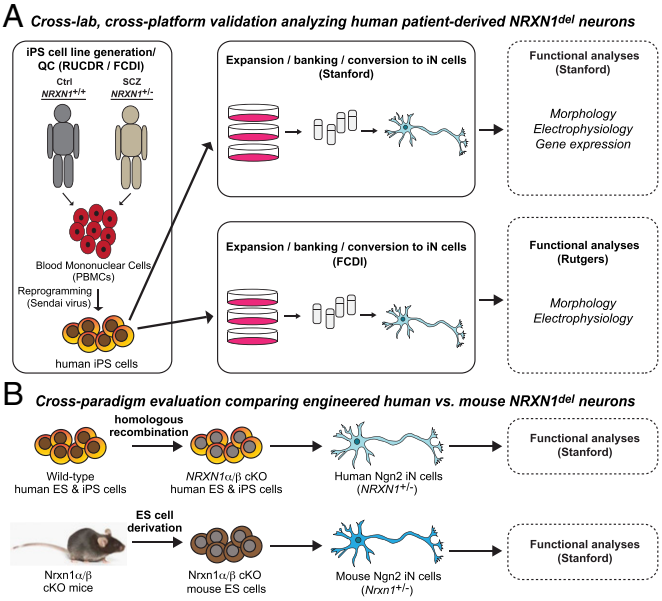

Fig. 1. Overall study design illustrating the experimental approach to analyze human heterozygous *NRXN1* loss-of-function mutations, to achieve cross-laboratory and cross-platform validation of observed phenotypes, and to perform cross-paradigm evaluations of these phenotypes in human and mouse neurons. (*A*) Experimental strategy for analyzing the functional effects of heterozygous *NRXN1* loss-of-function mutations in human patient-derived neurons and for validating the observed phenotypes in a cross-laboratory and cross-platform comparison. PBMCs from schizophrenia patients with *NRXN1* deletions and from control individuals were reprogrammed into iPS cells by Rutgers University (RUCDR Infinite Biologics). iPS cells that passed QC were shipped to Stanford and to FCDI for expansion, banking, and transdifferentiation into induced neurons. The indicated subsequent analyses were carried out at Stanford University and at Rutgers University. FCDI manufactured industry-scale human induced neurons that were shipped to Rutgers for analysis, whereas Stanford generated induced neurons at an academic single-laboratory scale for analysis. (*B*) Experimental strategy to evaluate the conservation of *NRXN1*-deletion phenotypes observed in human neurons in mouse neurons (cross-paradigm evaluation). Human and mouse stem cells that carried heterozygous engineered conditional *NRXN1*/*Nrxn1* deletions were transdifferentiated into neurons by Ngn2 expression and analyzed using similar approaches to ensure comparability. In this approach, isogenic human and mouse neurons without or with *NRXN1*/*Nrxn1* deletions were compared to test whether side-by-side analysis of human and mouse neurons prepared by indistinguishable approaches yields similar phenotypes.

via doxycycline. However, we observed unexpected differences between iPS cell lines. Every iPS cell line pair had to be optimized separately to achieve workable conditions for the induction, differentiation, and survival of Ngn2-induced neurons (*SI Appendix*, Fig. S2). Adjustments of lentivirus titers, starting cell numbers, and timing of the window of doxycycline application before puromycin selection were made for each iPS cell line, and no standard treatments with reliable survival and transdifferentiation of iPS cell lines into neurons was possible. This variability likely reflects clonal differences in iPS cell lines that are not immediately apparent in standard assays.

Although lentiviral Ngn2-induced transdifferentiation of iPS and ES cells into neurons is reproducible and reliable in an individual laboratory setting, it is not well suited for up-scaling. Therefore, FCDI optimized a large-scale manufacturing strategy to produce Ngn2-induced human neurons via the PiggyBac transposon system (*Materials and Methods*). This system utilizes stable transgene integration by PiggyBac that contains an inducible Ngn2 and a constitutive puromycin expression cassette. Puromycin-resistant cells were selected and expanded prior to doxycycline induction. Next, cryopreservation of Ngn2-induced human neurons was optimized, such that postmitotic neurons can be cryopreserved in a fashion where they retain their precryopreservation phenotype after thawing, and batches of cryopreserved human neurons were benchmarked against fresh cultures (*Materials and Methods*). Finally, postthaw culture conditions were optimized so that Ngn2-induced human neurons could be cultured long-term in any laboratory CO_2 incubator under defined media conditions and yield electrically and synaptically functional human neurons for imaging and whole-cell patch-clamp electrophysiology experiments (*Materials and Methods*).

Heterozygous *NRXN1* Deletions (*NRXN1*^{del}) Predisposing to Schizophrenia Do Not Affect Neuronal Morphology or Synapse Numbers. We previously characterized the effect of conditional heterozygous *NRXN1* mutations on the molecular, cellular, and electrophysiological properties of human neurons (29). In these studies, *NRXN1*-mutant neurons were derived from engineered ES cells carrying conditional heterozygous *NRXN1* deletions or truncations that could be induced by recombinases. We found that that *NRXN1* mutations did not impair dendritic arborization or synapse formation of human neurons, nor did they alter their passive membrane properties or action potential generation properties (29). Therefore, we tested the same parameters in Ngn2-induced neurons generated from pairs of schizophrenia patient-derived *NRXN1*^{del} and control iPS cells. Neurons were either generated with the small-scale method and analyzed at Stanford University, or were generated by the PiggyBac-based large-scale method at FCDI and analyzed at Rutgers University (Fig. 1*A* and *SI Appendix*, Fig. S2).

In two pairs of *NRXN1*^{del} and control neurons, we did not detect any significant changes in neurite outgrowth, number of primary dendritic processes, or dendritic branch points, or soma size (Fig. 2 *A* and *B* and *SI Appendix*, Fig. S3). Moreover, the density and size of synapses were not altered in *NRXN1*^{del} neurons (Fig. 2 *C* and *D* and *SI Appendix*, Fig. S3). Interestingly, despite different Ngn2-dependent neuronal induction strategies (lentiviral transduction vs. PiggyBac; laboratory vs. industrial), different laboratories (Stanford vs. Rutgers), and independent analytical strategies (IntelliCount semiautomated quantification vs. Metamorph counting), we consistently observed no deficit in synapse formation in *NRXN1*^{del} neurons (*Materials and Methods* and *SI Appendix*, Fig. S3) (29, 36). Thus, similar to previously examined engineered *NRXN1* mutations, patient-derived neurons with *NRXN1*^{del} CNVs do not display major morphological changes.

Schizophrenia-Associated *NRXN1*^{del} CNVs Do Not Significantly Alter the Intrinsic Membrane Properties of Neurons. Next, we investigated the electrical properties of schizophrenia patient-derived *NRXN1*^{del} neurons. Using patch-clamp recordings, we measured the membrane capacitance, input resistance, neuronal excitability, resting membrane potential, and various parameters of action potential generation in two pairs of *NRXN1*^{del} and control neurons. We detected no differences between schizophrenia patient-derived *NRXN1*^{del} neurons and corresponding control neurons in both pairs (*SI Appendix*, Fig. S4), suggesting that heterozygous loss of *NRXN1* does not affect nonsynaptic electrical properties of human neurons. Again, the data were consistent across the two different sites with neurons generated by different Ngn2 induction methods, providing a cross-platform validation of the results (*SI Appendix*, Fig. S4).

***NRXN1*^{del} CNVs Decrease the Frequency of Spontaneous Synaptic "Mini" Events.** To analyze synaptic function, we asked whether *NRXN1*^{del} neurons exhibit a change in spontaneous miniature excitatory postsynaptic currents (mEPSCs, monitored in the presence of tetrodotoxin) or spontaneous EPSCs (sEPSCs). Schizophrenia patient-derived *NRXN1*^{del} neurons exhibited a large (approximately

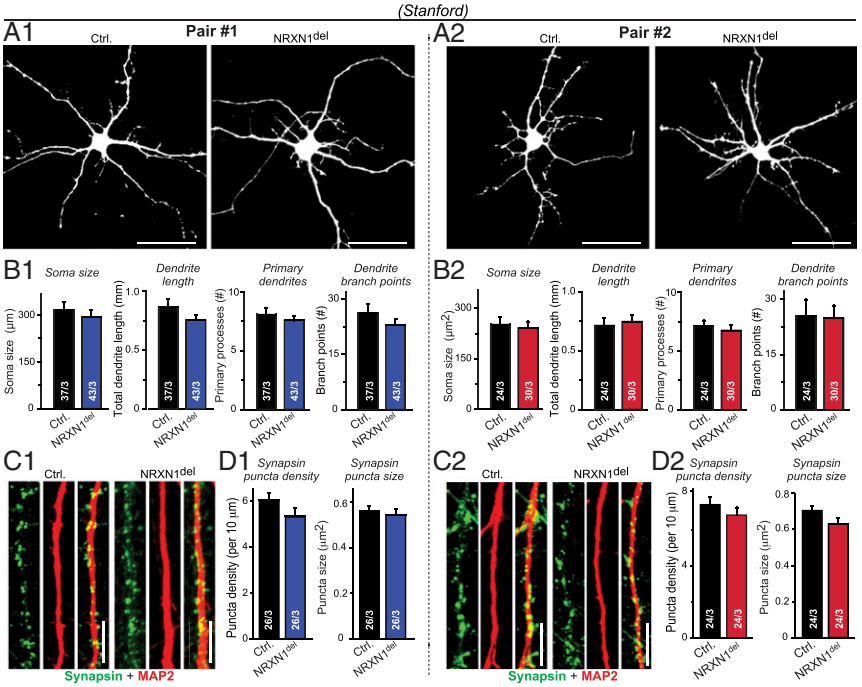

Fig. 2. Dendritic outgrowth and synapse formation are not significantly altered in *NRXN1*^{del} neurons transdifferentiated from iPS cells derived from schizophrenia patients. (*A* and *B*) *NRXN1*^{del} neurons exhibit no changes in soma size or dendritic arborization as analyzed at Stanford University in neurons obtained from two pairs of patient-derived vs. control iPS cells. (*A1* and *A2*) Representative confocal images of sparsely transfected cells expressing EGFP to label individual neurons for morphometric analyses. (Scale bars, 50 μm.) (*B1* and *B2*) Summary graphs of soma size, dendrite length, number of primary dendrites, and dendritic branch points. Neurons were analyzed at 4 wk in culture. (*C* and *D*) *NRXN1*^{del} neurons display no apparent change in synapse formation, assessed by the presynaptic marker Synapsin-1 as analyzed at Stanford University in two pairs of patient-derived vs. control neurons. (*C1* and *C2*) Representative confocal images of MAP2^{+} dendritic segments and Synapsin-1^{+} synapses. (Scale bars, 5 μm.) (*D1* and *D2*) Summary graphs of the density and size of Synapsin-1^{+} puncta measured on secondary dendrites in control and schizophrenia-associated *NRXN1*^{del} neurons. Data are means ± SEM (numbers in bars represent number of cells/experiments analyzed). Statistical analyses by Student's *t* test comparing *NRXN1*^{del} neurons to controls revealed no significant differences. For analyses performed at Rutgers University, see *SI Appendix*, Fig. S3.

twofold) decrease in mEPSC frequency, but no change in the mEPSC amplitude (Fig. 3). This decrease was observed in two independent pairs of *NRXN1*^{del} vs. control neurons. The decrease was similar in small-scale neurons produced and analyzed at Stanford University, and in large-scale neurons produced at FCDI and analyzed at Rutgers (Fig. 3). These results again phenocopy those previously obtained for engineered *NRXN1*-mutant human neurons (29), suggesting that the heterozygous *NRXN1* mutation impairs synaptic transmission.

Schizophrenia-Associated *NRXN1*^{del} CNVs Decrease the Neurotransmitter Release Probability. To determine whether the decrease in mEPSC frequency reflects a decrease in synaptic strength, and to determine whether this decrease may be caused by a change in neurotransmitter release probability, we measured action potential-evoked EPSCs mediated by α-amino-3-hydroxy-5-methyl-4-isoxazolepropionic acid receptors (AMPARs). Consistent with the decrease in mEPSC frequency, we observed a large decrease (approximately twofold) in EPSC amplitude in *NRXN1*^{del} neurons compared with controls. This decrease was detected in the two pairs studied above, and replicated with a third pair of *NRXN1*^{del} vs. control neurons (Fig. 4*A*).

We then examined whether the decreased synaptic strength in *NRXN1*^{del} neurons is due to a decrease in release probability, since the lack of a change in mEPSC amplitudes suggested that postsynaptic AMPARs were normal. We measured the coefficient of variation (CV) of evoked EPSCs, which is inversely proportional to the release probability (37). The CV of EPSCs was increased significantly (~1.4-fold) in *NRXN1*^{del} vs. control neurons, consistent with a decrease in release probability (Fig. 4*A*). To independently test this conclusion, we measured the paired-pulse ratio (PPR) of EPSCs, which is the ratio of the EPSC amplitudes evoked by two closely spaced action potentials. The PPR depends on the release probability because the extent of release induced by the first action potential determines, among others, how much additional release can be induced by a second action potential (38, 39). In control neurons, the PPR exhibited a decrease in the second response (referred to as paired-pulse depression) because the release probability under our recording conditions is high (Fig. 4*B*). However, in the *NRXN1*^{del} neurons generated from patient-derived iPS cells, paired-pulse depression was decreased, confirming a deficit in the initial release probability. This decrease in paired-pulse depression was replicated in all three pairs of *NRXN1*^{del} vs. control neurons at Stanford University (Fig. 4*B*).

We performed similar experiments with the two of the three pairs of *NRXN1*^{del} and control neurons (the same analyzed above) at Rutgers University, with comparable results (Fig. 4 *C* and *D*). Again, we observed a decrease in the EPSC amplitude and an increase in the CV of EPSCs, although the difference was not statistically significant (Fig. 4*C*). Moreover, we detected a significant decrease in paired-pulse depression (Fig. 4*D*). Taken together, these results indicate that patient-derived *NRXN1*^{del} neurons exhibit a robust and reproducible decrease in neurotransmitter release probability.

A Newly Engineered Conditional *NRXN1*^{del} iPS Cell Line Reproduces the Synaptic Impairments Observed in Patient-Derived *NRXN1*^{del} Neurons. In analyzing patient-derived neurons, a pressing question is whether the observed phenotypes in neurons with disease-associated CNVs or mutations are truly caused by these genetic changes, or are produced by the polygenic effects of a combination of specific mutations with a particular genetic background (31). Mutations associated with neuropsychiatric disorders often predispose to multiple disease conditions. For example, *NRXN1* CNVs are among the most frequent mutations associated not only with schizophrenia, but also with intellectual disability, autism spectrum disorders, and epilepsy (11, 13, 14, 40–45). We thus decided to test whether the similarity of the synaptic impairments we observed in *NRXN1*^{del} neurons generated from schizophrenia patient-derived iPS cells to those we previously described for *NRXN1*-deficient neurons generated from ES cells could be validated with neurons generated from iPS cells carrying a newly engineered conditional *NRXN1* mutation. For this purpose, we generated a new iPS cell line (from our control line C3141a) (*SI Appendix*, Table S1) carrying a heterozygous conditional knockout (cKO) of *NRXN1* using a strategy that is identical to the approach we previously employed in mice and in human ES cells (*SI Appendix*, Fig. S5 and Table S2). We produced this additional validation tool not only to test our conclusions, but also to generate a conditionally mutant *NRXN1* iPS cell line that can be freely

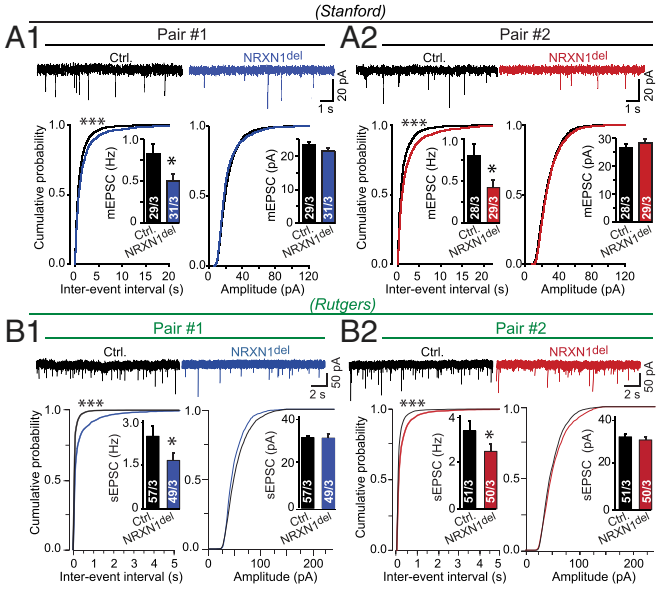

Fig. 3. *NRXN1*^{del} neurons transdifferentiated from schizophrenia patient-derived iPS cells exhibit a significant decrease in the frequency of spontaneous excitatory synaptic events. (*A*) The frequency but not amplitude of spontaneous mEPSCs is decreased approximately twofold in *NRXN1*^{del} neurons derived from schizophrenia patients compared with controls (*A1* and *A2*) (*Top*, representative traces of mEPSC recordings; *Bottom Left*, cumulative probability plots of interevent intervals and summary graphs of the mEPSC frequency; *Bottom Right*, cumulative probability plots and summary graphs of the mEPSC amplitude). mEPSCs were recorded in the presence of tetrodotoxin (TTX, 1 μM) at Stanford University. (*B*) Similar to *A*, but sEPSCs were analyzed in the absence of TTX with an independently generated set of neurons at Rutgers University (cross-laboratory and cross-platform validation). Data are means ± SEM (numbers in bars represent number of cells/experiments analyzed). Statistical analyses were performed by Student's *t* test for the bar graphs, and by Kolmogorov–Smirnov tests for cumulative probability plots, comparing *NRXN1*^{del} with control neurons (**P* < 0.05, ****P* < 0.001; nonsignificant comparisons are not indicated). All recordings were performed from 6 wk after the start of differentiation.

distributed for further studies, and that is not subject to the commercial constraints imposed on the previously generated conditionally mutant *NRXN1* ES cell lines (29).

We limited our analysis of the newly engineered conditional *NRXN1*^{del} neurons to key measurements, namely assessments of mEPSCs and evoked EPSCs. The newly engineered *NRXN1*^{del} neurons exhibited the same decrease in mEPSC frequency, EPSC amplitude, and paired-pulse depression as patient-derived *NRXN1*^{del} neurons (Fig. 5 *A–C* and *SI Appendix*, Fig. S6 *A* and *B*). These results confirm that heterozygous *NRXN1* deletions produce a robust synaptic phenotype in human neurons, suggesting that the associations of heterozygous *NRXN1* deletions with specific neuropsychiatric disorders, such as schizophrenia, cannot be explained by the *NRXN1* deletion alone, and are likely shaped by factors downstream of the synaptic impairments. Since our newly engineered line was generated in an iPS cell line that can be distributed without commercial restrictions, this line is now available for further mechanistic and therapeutic studies in schizophrenia.

Mouse Neurons Carrying the Heterozygous *Nrxn1*^{del} Allele Do Not Recapitulate the Human *NRXN1*^{del} Phenotype. In our earlier analysis of the engineered conditional human *NRXN1*^{del} neurons, we found that dissociated cultures of mixed mouse neurons and glia obtained from the cortex of heterozygous or homozygous *Nrxn1α* KO mice did not replicate the heterozygous *NRXN1*^{del} phenotype (29). This appeared to indicate that human neurons are uniquely sensitive to the heterozygous deletion of *NRXN1*, which is unexpected given the apparent structural and functional similarity between human *NRXN1* and mouse *Nrxn1*. However, in these original experiments the compared human and mouse neurons were quite different. The mouse neurons were primary cultures of many cell types that were analyzed as a mixture derived from the mouse cortex after neurogenesis and neuronal migration had completed, whereas the human neurons constituted a relatively homogeneous population of directly converted neurons. Moreover, the mouse neurons were from *Nrxn1α* KO animals, whereas the human neurons carried heterozygous deletions of both *NRXN1α* and *NRXN1β*. Thus, these earlier experiments did not reveal whether or not heterozygous *Nrxn1* deletions in mouse neurons would produce a phenotype similar to that observed for the human neurons analyzed here.

To directly test whether human and mouse neurons are indeed differentially sensitive to heterozygous *NRXN1*/*Nrxn1* deletions, we repeated the precise experiment that we had performed with engineered human *NRXN1*^{del} neurons with the equivalent mouse *Nrxn1*^{del} neurons. For this purpose, we generated ES cells from mice with the same heterozygous mutation as the human conditional *NRXN1*^{del} iPS and ES cells (28, 46). We converted these mouse ES cells into Ngn2-induced neurons, and analyzed the electrophysiological phenotype of these neurons. Strikingly, the mouse neurons did not exhibit a significant synaptic impairment (Fig. 5 *D–F* and *SI Appendix*, Fig. S6 *C* and *D*). They displayed a normal mEPSC frequency, and a trend toward a decrease in EPSC amplitude that was not statistically significant (Fig. 5 *D–F*). Moreover, the mouse *Nrxn1*^{del} neurons showed no change in PPR, possibly the most sensitive electrophysiological phenotype (Fig. 5 *E* and *F*). These results indicate that the synaptic phenotypes conferred by the heterozygous human *NRXN1*^{del} mutations are unique to the human neuronal context.

Heterozygous *NRXN1* Deletions Consistently Increase CASK Protein Levels in Human Neurons. One striking finding previously obtained in ES cell-engineered *NRXN1*^{del} neurons was the increase in CASK protein stability, which was detected with two different engineered *NRXN1* mutations (29). CASK is a cytoplasmic scaffolding protein that interacts with neurexins (47) and forms a tight complex with other presynaptic proteins (48–52). In human patients, mutations in *CASK*, which is X-linked, are associated with autism spectrum disorders and X-linked mental retardation in addition to brain malformations (53–58). We thus tested whether CASK protein is also increased in schizophrenia patient-derived *NRXN1*^{del} neurons. Consistent with previous studies, we observed a large increase (>50%) in CASK protein levels in *NRXN1*^{del} neurons, while all other synaptic proteins measured were not altered, with the exception of *NRXN1* protein levels, which were down-regulated by ~50% (Fig. 6*A* and *SI Appendix*, Fig. S7*A*). Moreover, we detected a similar increase in CASK levels in neurons derived from the newly engineered heterozygous *NRXN1*^{del} iPS cell line (Fig. 6*B* and *SI Appendix*, Fig. S7*C*), further validating this change. Since no change in CASK mRNA levels was detected in the RNA-sequencing (RNA-seq) experiments (see next section), these results indicate that CASK protein is stabilized and protected from degradation upon heterozygous deletion of *NRXN1* in human neurons.

***NRXN1*^{del} Neurons Exhibit Modest Changes in Gene Expression.** Using 4-wk-old, relatively mature human neurons generated from the three pairs of patient-derived *NRXN1*^{del} and control iPS cells that we analyzed in Fig. 4, we performed bulk RNA-seq on total RNA in triplicate (Fig. 7*A*). In addition, we performed RNA-seq analyses (in triplicate) on isogenic pairs of human neurons without or with the heterozygous *NRXN1* deletion that were transdifferentiated from the newly engineered iPS cell line carrying a conditional *NRXN1*^{del} allele (Fig. 5 and *SI Appendix*, Fig. S5), and on three unrelated wild-type iPS cell lines (in duplicate). In total,

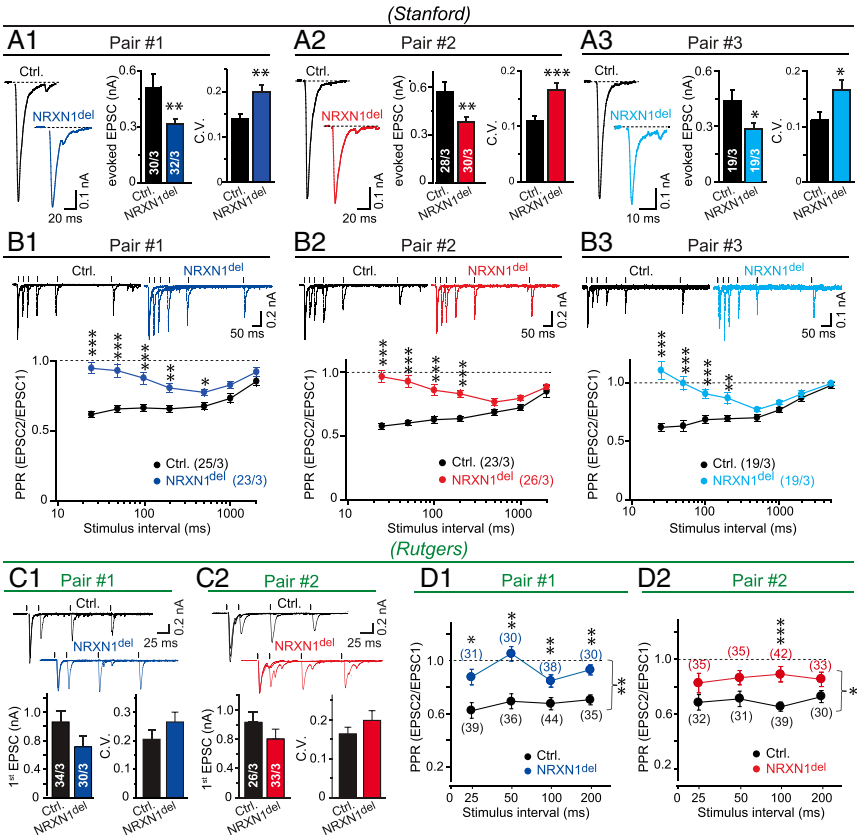

Fig. 4. Evoked excitatory synaptic transmission is impaired in *NRXN1*^{del} neurons transdifferentiated from patient-derived iPS cells due to a decrease in release probability. (*A*) *NRXN1*^{del} neurons display an ~30 to 40% decrease in the amplitude of evoked AMPAR-mediated EPSCs along with an increase in the CV of evoked EPSC amplitudes in Pair #1 (*A1*), Pair #2 (*A2*), and Pair #3 (*A3*) of control and schizophrenia *NRXN1*^{del} neurons, as analyzed at Stanford University (*A1–A3*: separate analyses of the three pairs of patient-derived vs. control neurons; *Left*, representative traces of evoked EPSCs; *Center* and *Right*, summary graphs of the EPSC amplitude and CV). (*B*) *NRXN1*^{del} neurons display a significant increase in the PPR of evoked AMPAR-mediated EPSCs compared with matched control neurons, as analyzed at Stanford University (*B1–B3*: separate analyses of the three pairs of patient-derived vs. control neurons; *Top*, representative traces of PPR recordings, only the first five interstimulus interval is shown [25 to 500 ms] and stimulus artifacts are removed for better overview; *Bottom*, summary plots of PPR as a function of the interstimulus intervals in the range of 25 to 5,000 ms). (*C* and *D*) *NRXN1*^{del} neurons derived from schizophrenia patients exhibit trend toward a decrease in the amplitude of evoked EPSCs and a significant increase in the PPR of EPSCs when compared with matched controls, as analyzed at Rutgers University for two patient-control pairs. (*C*, *Top*) Representative traces of EPSCs recorded in response to two sequential action potentials elicited with 25- to 200-ms intervals. (*Bottom*) Summary graphs of the amplitude and CV of the first EPSC response evoked by the first of the two sequential action potentials. (*D*) Summary plot of the PPR of EPSCs elicited with 25- to 200-ms intervals). Data are means ± SEM (numbers in bars represent number of cells/experiments analyzed). Statistical analyses were performed by Student's *t* test for the bar graphs (*A* and *C*) and by two-way RM ANOVA with Tukey's post hoc test for summary plots (*B* and *D*), comparing *NRXN1*^{del} neurons with controls (**P* < 0.05; ***P* < 0.01; ****P* < 0.001; nonsignificant comparisons are not indicated). Neurons were analyzed at 6 wk in culture.

we analyze 30 samples (9 control and schizophrenia-*NRXN1* mutants, 3 controls and engineered *NRXN1* mutants, and 6 wild-type iPS cell samples; replicates are from independent cultures at different time points).

Since human neurons are cocultured with mouse glia, the RNA-seq data constituted a mixture of human neuronal and mouse glia transcriptomes. Thus, we needed to deconvolve the two transcriptomes and normalize the relative abundance of each species' mRNA to the total number of that species' mRNAs (*Materials and Methods*). The Kallisto program unambiguously assigned each paired 150-bp sequence to mouse and human reference transcriptomes (59). Since mouse:human mRNA ratios differed between cultures of neurons transdifferentiated from various iPS cell lines, we adjusted each sample's species-specific mRNA abundance based on transcripts per million (TPM) for each gene, summed these for each gene, and then carried out per sample quantile normalization steps (60) (Fig. 7*A*). This approach provided a reproducible abundance measure for each gene per sample. The resulting values were used to form a $\log_2$(TPM+1) gene-by-sample matrix that was used for differential gene-expression analyses.

As described above, our samples included three types of reprogrammed cells: induced neurons generated from iPS cell lines from patient and control donors; isogenic neuronal cultures generated from an engineered iPS cell line carrying a conditional heterozygous NRXN1del knockout construct; and wild-type iPS cells. To gain a better understanding of the transcriptomic state of our cultures, we selected 7,763 differentially expressed genes (DEGs) from the RNA-seq datasets that met at least one of the following four criteria in *t* tests comparing different types of cells: an absolute value of $t \geq 15$ in comparisons of engineered vs. iPS cells, of nonengineered vs. iPS cells, or of induced neurons in general vs. iPS cells; or an absolute value of $t \geq 4$ for engineered vs. nonengineered neurons. These tests used the *limma-trend* procedure (*Materials and Methods*). *K*-means cluster analysis of these DEGs revealed 11 clusters; these were reduced to 7 clusters based on similarity (Fig. 7*B* and *SI Appendix*, Fig. S8*C*). Analyses of functional enrichment of gene ontology (GO) categories (*Materials and Methods*) suggested that different clusters were associated with distinct biological categories, but could not be assigned to defined functional biological pathways. For example, clusters C1 and C3 are both associated with "synaptic signaling" and "presynapse," whereas clusters C6 and C7 are both associated with "nucleic acid binding."

Principal component analysis of the transcriptome identified, as expected, the most significant gene-expression differences between those of iPS cells vs. induced neurons (*SI Appendix*, Fig. S8 *A* and *B*), consistent with the profound gene-expression changes induced by transdifferentiation of iPS cells into neurons (30, 61–63). The second most significant gene-expression differences were detected between the transcriptomes of neurons derived from control and patient-derived *NRXN1*^{del} iPS cells vs. neurons derived from engineered iPS cells (independent of whether they were *NRXN1*^{del} or wild-type neurons) (Fig. 7 and *SI Appendix*, Fig. S8 *A* and *B*). Nonengineered iPS cell-derived neurons exhibited a more mature neuronal gene-expression signature compared with neurons from engineered iPS cells (Flp vs. Cre). Because of this difference, subcomparisons (e.g., comparing wild-type neurons from control vs. engineered iPS cells) also uncovered significant differences in gene expression. The large transcriptome differences between neurons from engineered vs. nonengineered neurons is unexpected because the engineered iPS cells were derived from one of the three control iPS cell lines, and thus "isogenic." Since engineered iPS cells were

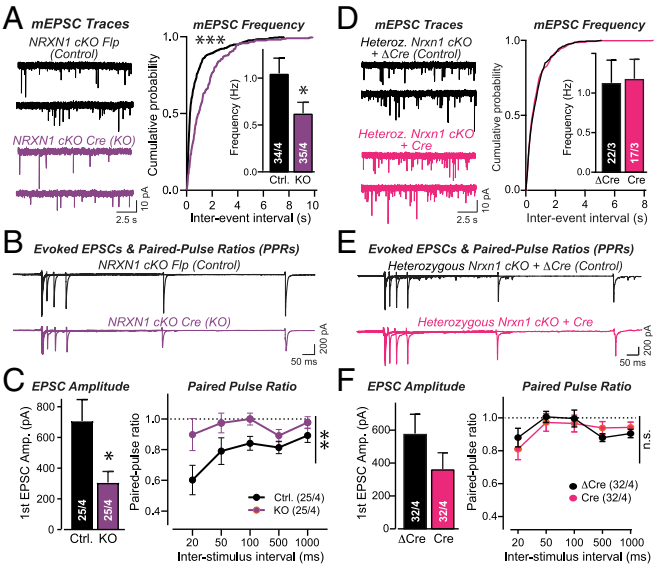

Fig. 5. Isogenic heterozygous deletion of human but not of mouse *NRXN1/Nrxn1* replicates the impairment in presynaptic release probability observed in *NRXN1*^{del} neurons transdifferentiated from schizophrenia patient-derived iPS cells. (*A*) Heterozygous *NRXN1*^{del} neurons generated from a newly engineered *NRXN1* cKO iPS cell line (1215sub) exhibit a large decrease in mEPSC frequency but not mEPSC amplitude (*Left*, sample traces of mEPSCs; *Right*, cumulative probability plot of the mEPSC interevent intervals and summary graph of the mEPSC frequency). Neurons were infected with lentiviruses expressing Flp (creates wild-type genotype [black]) or Cre (induces heterozygous *NRXN1* KO [purple]). (*B*) Sample traces of evoked EPSCs elicited by closely spaced pairs of action potentials (intervals: 20 ms, 50 ms, 100 ms, 500 ms, 1,000 ms) to measure both the EPSC amplitude and the EPSC PPR from neurons derived from the *NRXN1* cKO iPS cell line. (*C*) Conditional heterozygous *NRXN1* deletion in engineered neurons induces a greater than twofold decrease in the amplitude of evoked EPSCs (*Left*, summary graph of the amplitude of the first evoked EPSC) and a greater than twofold reduction in the paired-pulse depression of evoked EPSCs (*Right*, summary plot of the PPR, measured as the amplitude ratio of the second over the first evoked EPSC, and plotted as a function of the interstimulus interval). Data are means ± SEM; numbers of cells/cultures analyzed are shown in the bar diagrams. Statistical significance was evaluated with the Kolmogorov–Smirnov test (cumulative probability plots), one-tailed *t* test (summary graphs), or two-way ANOVA (PPR plots) (*$P < 0.05$; **$P < 0.01$, ***$P < 0.001$). All recordings were performed from 6-wk-old neurons. (*D*) Heterozygous *Nrxn1* deletions in mouse neurons cause no significant changes in mEPSC frequency. ES cells isolated from heterozygous *Nrxn1* cKO mice (27) were transdifferentiated into neurons using Ngn2 expression, infected with lentiviruses expressing Cre (to induce the heterozygous *Nrxn1* deletion) or ΔCre (control), and analyzed at day in vitro 14 to 16 (*Left*, representative mEPSC traces; *Right*, cumulative probability plots of the mEPSC interevent intervals; *Inset*, summary graph of the mEPSC frequency). (*E* and *F*) Heterozygous *Nrxn1* deletions in mouse neurons also cause no significant impairments in evoked synaptic transmission. EPSCs were recorded in response to two sequential stimuli separated by defined interstimulus intervals (20 ms, 50 ms, 100 ms, 500 ms, 1,000 ms) in neurons prepared as described in *D*. (*E*) Representative traces. (*F*, *Left*) Summary graph of the amplitude; (*Right*) summary plot of the PPR of the EPSCs displayed as a function of the interstimulus intervals. Numerical data are means ± SEM (number in bars or brackets show number of cells/cultures analyzed). No significant differences were detected between test and control conditions using an unpaired, one-tailed *t* test (*D*) or a two-way ANOVA (*E*).

subjected to stringent quality controls, such as karyotyping (*SI Appendix*, Fig. S1*B*), the transcriptome differences are not due to large chromosomal arrangements. The process of subcloning and engineering iPS cells thus may be sufficient to produce large shifts in the properties of iPS cells and neurons derived from these lines. On the background of these gene-expression differences, the strong similarity in the synaptic phenotypes of patient-derived and engineered *NRXN1*^{del} neurons appears compelling.

A primary goal of the bulk RNA-seq experiments was to assess the effect of heterozygous *NRXN1* deletions on gene transcription. Surprisingly, however, we observed no consistent differences between *NRXN1*^{del} and control neurons in principal component analyses (*SI Appendix*, Fig. S8 *A* and *B*). None of the DEG clusters was driven by gene-expression differences between *NRXN1*^{del} vs. wild-type neurons (Fig. 7*B* and *SI Appendix*, Fig. S8*C*). These observations indicate that the heterozygous *NRXN1* deletion does not produce major perturbations of gene expression, but do not rule out more subtle effects. To achieve a more granular analysis, we selected (after initial QC, see *Materials and Methods*) 12,910 genes with expression values ≥2 in at least one of 18 patient and control samples, and >0.1 in all 18. We analyzed these genes using a moderated paired *t* test (with *limma-trend*), pairing the patient and control replicates that were cultured in the same plate at the same time, to identify DEGs with the highest significance.

First, we examined the most strikingly dysregulated genes (see Datasets S1–S4 for detailed results). No *P* values were significant after Bonferroni correction, and only 15 DEGs achieved a Benjamini and Hochberg false-discovery rate (FDR) of 30%. We constructed a volcano plot highlighting 78 genes with an uncorrected $P \leq 0.001$ and a $|\log_2(\text{fold-change})| \geq 0.8$ (*SI Appendix*, Fig. S9*A*) to consider whether any gene-expression changes were plausibly caused by the *NRXN1* deletion (*SI Appendix*, Fig. S9 *B* and *C*). No obvious functional signature emerged from these DEGs. For example, although the heterozygous *NRXN1* deletion produced a selective and large impairment in synaptic transmission, only two genes among the top DEGs encode specifically synaptic proteins (CPLX2 and C1QL3), both of which are down-regulated (*SI Appendix*, Fig. S9*A*). *CASK* expression is not significantly up-regulated in *NRXN1*^{del} neurons, confirming previous data that *CASK* protein levels are up-regulated posttranscriptionally in *NRXN1*^{del} neurons (29).

Second, we selected test sets of 296 down- and 403 up-regulated DEGs for *NRXN1*^{del} vs. control neurons, using a broader set of criteria [uncorrected $P < 0.05$ and $|\log_2(\text{fold-change})| > 2$]. We annotated these DEGs in a GO analysis with the ToppFun function of ToppGene (https://toppgene.cchmc.org) (*Materials and Methods* and Datasets S1–S4). We used hypergeometric tests to compare the fraction of the test set (11,880 post-QC genes for this enrichment analysis) that was associated with a given GO term with the fraction of the up- and down-regulated DEGs associated with the same term. No GO terms for up-regulated DEGs were significant after Bonferroni or FDR correction. For down-regulated DEGs, multiple terms in all three GO categories exhibited a Bonferroni-corrected significant enrichment of DEGs compared with the test set. Characteristic top terms are listed in *SI Appendix*, Fig. S9*D* (see also Datasets S1–S4). The up-regulated genes notably included *KYAT3* that encodes kynurenine aminotransferase 3, while the down-regulated genes included RELN (involved in neuronal development and signaling) and transcription factors such as TBX1 (*SI Appendix*, Fig. S9 *A–C*). The increase in KYAT3 expression was highly reproducible in various experiments, suggesting a true expression change (*SI Appendix*, Fig. S9*B*). Quantitative immunoblotting experiments confirmed an increase in KYAT3 protein levels, supporting the mRNA expression results (Fig. 6*A* and *SI Appendix*, Fig. S7*B*).

qRT-PCR Suggests that Increased *NNAT* Expression Is an Intrinsic Property of Patient-Derived *NRXN1*^{del} iPS Cells. In the RNA-seq experiments, genes were excluded from analyses if one or more of the 18 samples had an expression value of ≤0.1. One of these genes, *NNAT* (encoding neuronatin), demonstrated a striking up-regulation in neurons derived from *NRXN1*^{del} patients but not in engineered *NRXN1*^{del} neurons. qRT-PCR experiments on patient-derived *NRXN1*^{del} vs. control neurons confirmed that *NNAT* expression was massively enhanced in patient-derived *NRXN1*^{del} neurons (*SI Appendix*, Fig. S9 *E–G*). Other neuronal control genes exhibited no

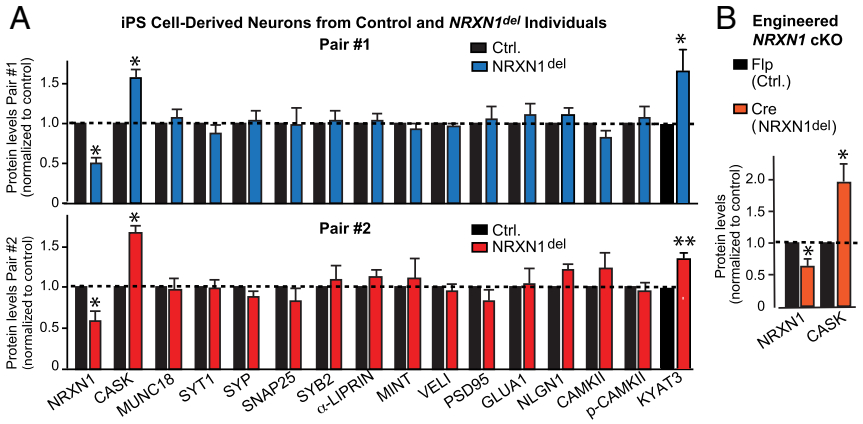

Fig. 6. CASK protein levels are up-regulated in *NRXN1*^{del} neurons generated from schizophrenia patient-derived iPS cells and from genetically engineered iPS cells. (*A*) Quantifications of protein levels in the two pairs of *NRXN1*^{del} and control neurons reveal that apart from a large increase in CASK protein levels and a decrease in neurexin levels, no other major changes were detected in the levels of the analyzed proteins. All analyses were carried out using quantifications with fluorescently labeled secondary antibodies and TUJ1 as a loading control. For representative corresponding blots, see *SI Appendix*, Fig. S7. (*B*) Quantifications reveal that the engineered conditional *NRXN1* deletion in an iPS cell background (1215sub) also causes an increase in CASK protein levels. Experiments were performed as in *A*. Data are means ± SEM (n = 3 to 5 independent cultures). Statistical analyses were performed by Student's t test comparing test samples with the control (*P < 0.05, **P < 0.01).

increase except for a small but significant increase in *RIMS1* expression (*SI Appendix*, Fig. S9 *E–G*). Moreover, *NNAT* mRNA levels were also consistently increased in patient-derived *NRXN1*^{del} iPS cells when compared with control iPS cells (*SI Appendix*, Fig. S9*H*).

Could the increased *NNAT* expression be directly caused by the *NRXN1* deletion? *NRXN1*^{del} neurons obtained from two different engineered, conditionally mutant stem cell lines [the original ES cell line (29)] (*SI Appendix*, Fig. S9*I*) and the newly engineered iPS cell line (*SI Appendix*, Fig. S9*J* and Table S2) exhibited no increase in *NNAT* expression, even though they displayed the modest increase in *RIMS1* expression observed in patient-derived *NRXN1*^{del} neurons (*SI Appendix*, Fig. S9 *I* and *J*). Thus, *NRXN1*^{del} neurons and iPS cells derived from schizophrenia patients exhibited a consistent *NNAT* expression change that was absent from controls and "normal" neurons in which the same *NRXN1* deletion was engineered, despite the fact that these neurons displayed the same functional phenotypes. A possible reason for the difference in *NNAT* expression between the engineered *NRXN1*^{del} and the patient-associated *NRXN1*^{del} mutation could be that *NNAT* is an imprinted gene (64, 65). Silencing of *NNAT* by imprinting may be maintained in the engineered iPS cell line but not in the patient-derived iPS cell line. Alternatively, the relative immaturity of the engineered neurons may be responsible, but this seems unlikely because *NNAT* expression is already increased in patient-derived *NRXN1*^{del} iPS cells and thus independent of neuronal transdifferentiation and maturation.

Discussion

Schizophrenia is a devastating and prevalent mental disorder with a huge impact on millions of patients and their families. Recent advances in human genetics have identified variations in multiple chromosomal regions and genes that contribute to the genetic risk for schizophrenia and may provide clues to schizophrenia pathogenesis (4, 9). Enormous progress was made in describing the genetic landscape underlying schizophrenia, resulting in the realization that changes in a large number of genes contribute to schizophrenia (7, 15–17, 66, 67). This genetic heterogeneity supports the notion that schizophrenia is a multifactorial disorder that may not be induced by a general pathophysiological mechanism but result from diverse molecular changes.

Among CNVs predisposing to schizophrenia, 2p16.3 CNVs are notable in that they affect expression of only a single gene, *NRXN1* (7, 14). *NRXN1* CNVs at 2p16.3 strongly predispose to schizophrenia, but also to other neuropsychiatric disorders, affecting thousands of patients. *NRXN1* CNVs are at present the most prevalent known single-gene mutation associated with schizophrenia, although other CNVs involving multiple genes (such as 22q11.2) are more prevalent (7, 10, 11). Strikingly, our previous study suggested that heterozygous deletions of *NRXN1* in human but not in mouse neurons cause a distinct and robust impairment in neurotransmitter release without changing the development or the morphology of neurons (29). This was an exciting finding because it identified a robust phenotype caused by a schizophrenia-associated mutation that could potentially be used to gain insight into schizophrenia pathophysiology and may even be amenable for drug development. Given the current reproducibility crisis, however, it was necessary to independently assess these results. Thus, the present study aimed for a multidimensional validation of these findings. Specifically, the present study had five objectives: 1) to validate or refute the results obtained with engineered conditionally mutant ES cells, using patient-derived iPS cells with a similar mutation; 2) to confirm that the observed phenotype is independent of a particular laboratory (i.e., that it can be replicated at multiple sites); 3) to generate tools and reagents for general use by the scientific community to study the cellular basis of neuropsychiatric disorders; 4) to determine whether human neurons are uniquely sensitive to a heterozygous loss of *NRXN1* as compared with mouse neurons; and 5) to achieve further insights into the mechanisms by which *NRXN1* mutations may predispose to schizophrenia. The present study achieved all of these objectives.

We show that human neurons derived from patients with a heterozygous *NRXN1* deletion (*NRXN1*^{del} neurons) exhibit the same phenotype of synaptic impairments as engineered human neurons with a heterozygous *NRXN1* deletion, and that this phenotype is robustly observed in different laboratories (Figs. 2–4 and 6). This result validates the generality of the synaptic phenotype we described earlier, demonstrating that it is disease-relevant (objectives 1 and 2). Moreover, we engineered a conditional *NRXN1*^{del} iPS cell line that is free from commercial restrictions for general use by the scientific community, and that enables production of human neurons with a conditional *NRXN1* deletion exhibiting a phenotype identical to that of patient-derived *NRXN1*^{del} neurons (Fig. 5) (objective 3). Furthermore, only human but not mouse *NRXN1*^{del} neurons prepared by the same neuronal induction protocol from stem cells exhibited a robust phenotype of synaptic impairments (Fig. 5). This result indicates that at least some genes predisposing to human neuropsychiatric disorders should preferentially be analyzed in human neurons (objective 4). Overall, our results therefore establish that in human neurons, heterozygous *NRXN1* deletions, independent of whether they result from spontaneous CNVs or genetic engineering in stem cells, produce a robust but discrete functional phenotype that consists of a decrease in release probability without a change in synapse numbers or neuronal development.

The definition of this synaptic impairment enables a mechanistic approach to a better understanding of schizophrenia pathophysiology in patients with *NRXN1* mutations. Besides establishing *NRXN1*^{del} neurons as a robust model system for future studies, our

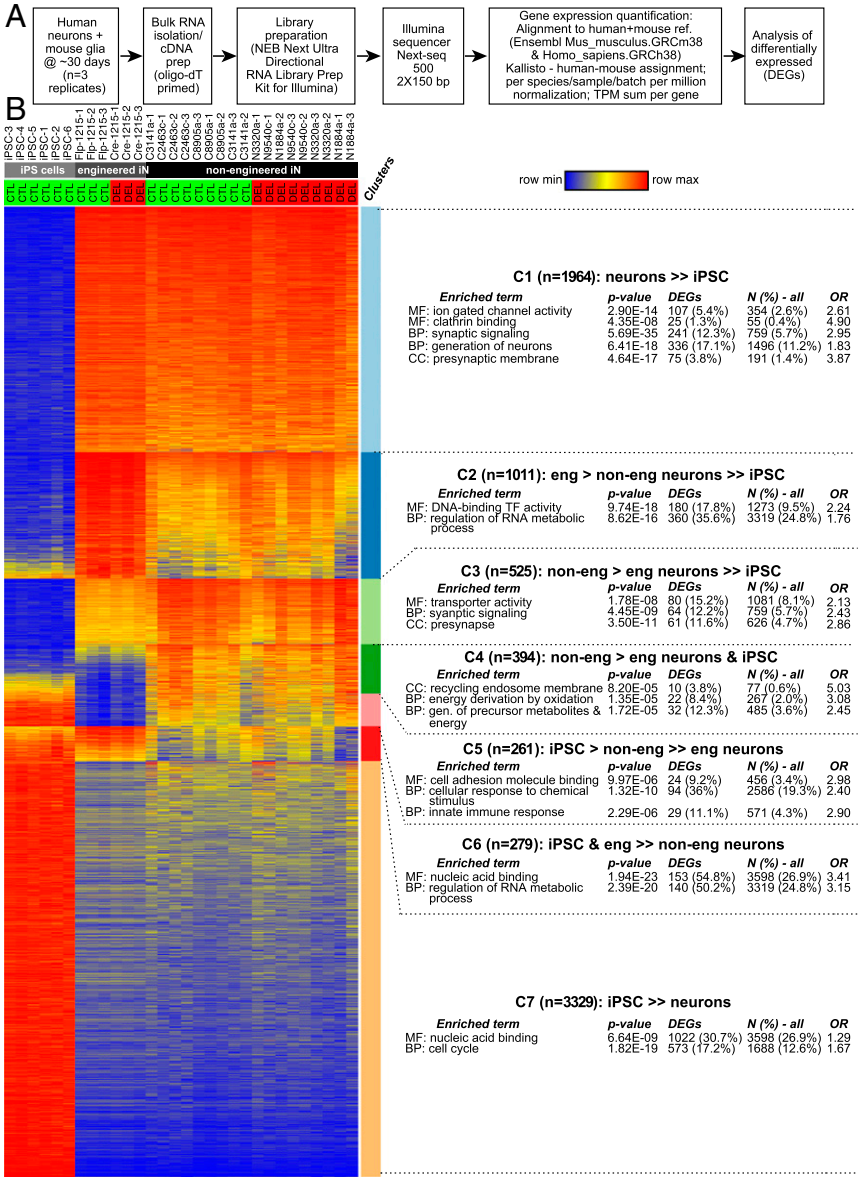

Fig. 7. RNA-seq analyses comparing the transcriptomes of control iPS cells and of *NRXN1*^{del} and control neurons reveal distinct patterns of differential gene expression. (*A*) Flow-diagram of bulk RNA-seq experiments. Genes for analyses were selected from 17,004 gene IDs with $\log_2(\text{TPM}+1) \geq 2$ in at least 1 of the 30 samples. (*B*) Cluster analysis of DEGs. The heat map shows the relative expression level of each gene for each culture. The annotation lists results for selected terms with the most significant *P* values for each Cluster: the *P* value; the number and percentage of cluster DEGs and of all test set genes assigned to the term, and the odds ratio (OR). Because GO categories annotate the same genes multiple times, the 5% α-level for Bonferroni correction considered the number of tested terms in each category separately (MF: 1,209, $P = 4.14E\text{-}05$; BP: 6,405, $P = 7.81E\text{-}06$; CC: 846; 5.91E-05). For details, see *SI Appendix, Detailed Experimental Procedures*.

results provide information on pathogenetic mechanisms (Figs. 6 and 7) (objective 5). The electrophysiological studies revealed that *NRXN1*^{del} neurons exhibit a selective impairment in neurotransmitter release without changes in other neuronal properties, suggesting a circumscribed dysfunction of synaptic transmission that is related to the release machinery. Consistent with this conclusion, we uniformly detected in *NRXN1*^{del} neurons an increase in CASK protein levels, possibly because a decrease in *NRXN1* signaling via CASK may lead to a compensatory increase in CASK levels (Fig. 6). In the RNA-seq studies, few major changes in gene expression were detected, suggesting that *NRXN1* is not directly involved in regulating gene expression (Fig. 7). However, several interesting gene-expression changes were noted. In all patient-derived *NRXN1*^{del} neurons, we detected a significant up-regulation in *NNAT* expression. *NNAT* appears to perform a regulatory role in secretory tissues, especially the brain (68, 69). We did not detect an up-regulation of *NNAT* in *NRXN1*^{del} neurons derived from genetically engineered iPS cells, possibly because *NNAT* is an imprinted gene and the imprinting state may differ among iPS cells. The fact that *NNAT* is not increased in the engineered *NRXN1*^{del} neurons indicates that the increase in *NNAT* expression is not responsible for the synaptic phenotype that is uniformly observed in the patient-derived and engineered *NRXN1*^{del} neurons. Finally, the RNA-seq experiments identified a prominent change in the expression of *KYAT3* that mediates the biosynthesis of kynurenic acid. Kynurenic acid can act as an anticonvulsant, is an antagonist of ionotropic glutamate receptors, and has been proposed to be critically involved in schizophrenia pathogenesis (70). In particular, kynurenic acid is thought to suppress NMDA-receptor function, which in turn is also regulated by *NRXN1* (27) and may be decreased in schizophrenia (67, 71). Thus, an overall

picture emerges whereby *NRXN1* dysfunction might operate in the same pathway as kynurenic acid in schizophrenia pathogenesis.

How do the current results relate to other genetic predispositions to schizophrenia? The SCHEMA study recently identified ultrarare mutations in 10 genes (*SETD1A*, *CUL1*, *XPO7*, *TRIO*, *CACNA1G*, *SP4*, *GRIA3*, *GRIN2A*, *HERC1*, and *RG1CC1*) that strongly predispose to schizophrenia, with half of these genes having a larger effect size than *NRXN1* deletions, although being much less frequent (67). These genes appear to have very different functions and cannot be easily fitted into a single synaptic or nonsynaptic pathway. Most of these genes are incompletely understood, and it is possible that biological studies such as those performed here will uncover additional commonalities that are currently not anticipated. Interestingly, however, two of these genes encode proteins that are directly regulated by neurexins. The synaptic recruitment of NMDARs, including those containing the GRIN2A subunit, is controlled by NRXN1 (27), whereas the synaptic recruitment of AMPARs, including those containing the GRIA3 subunit, is controlled by NRXN3 (23). Together with the regulation of KYAT3 that is also part of the NMDAR-regulatory pathway, a picture emerges whereby incremental changes in postsynaptic glutamate receptor function in some circuits may predispose to schizophrenia.

In summary, we here present evidence that the robust synaptic phenotype observed upon *NRXN1* deletions in human neurons is disease-relevant since it is fully reproducible in patient-derived neurons. Moreover, in generating iPS cells with a conditional *NRXN1* deletion, we have produced a generally available resource for studying schizophrenia pathophysiology. Finally, we have shown that the heterozygous *NRXN1* deletion phenotype is not observed in mouse neurons under the same experimental conditions, strengthening the rationale for studying disease phenotypes in human neurons. The stage is now set to use these findings and reagents for insight into the molecular mechanisms involved.

Materials and Methods

Patient and Control Cohort. Case and control donors for this study are described in *SI Appendix*, Table S1. For the six individuals (three *NRXN1* deletion schizophrenia cases and three controls) for whom data are reported in this paper, 33 to 41× whole-genome DNA paired-end 150-bp sequencing (WGS) was carried out from genomic DNA extracted from whole blood. For details on patients and genomics, see *SI Appendix*.

iPS Cell Generation, Banking, and QC Procedures. $CD4^+$ T cells were obtained from frozen PBMC specimens and reprogrammed into iPS cells using the Sendai virus method at RUCDR Infinite Biologics. For details on QC and culture procedures, see *SI Appendix*.

Gene Targeting. The previously reported *NRXN1* cKO strategy for homologous recombination (29) was used to engineer the control C3141a iPS cell line using TALENs (FCDI engineering team). Multiple subclones were generated and tested for correct genomic integration by PCR and Sanger sequencing. Karyotyping, pluripotency test, mycoplasma test, and postthaw cell test were performed on the engineered lines. Cell lines were shipped on dry ice to multiple sites and viability, genotype, and differentiation were independently tested by individual laboratories (Stanford and University of Massachusetts). Cells were genotyped using previously described primers (29). For details, see *SI Appendix*.

FCDI iN Cell Methods. Engineered iPS cell lines were generated at FCDI using PiggyBac-mediated insertion of an inducible human *Ngn2* expression cassette alongside constitutive rtTet expression. For details, see *SI Appendix*,.

Lentiviruses were produced as described previously (29, 62). For details, see *SI Appendix*.

Generation of Human Neurons (iN Cells) from iPS Cells. Neurons were generated from iPS cells as described previously (30, 35). For details, see *SI Appendix*.

Analyses of Gene Expression Using RNA-seq and qRT-PCR. For bulk RNA-seq and qRT-PCR validations, total RNA was isolated and analyzed from 4- to 4.5-wk-old neurons cocultured with mouse astrocytes as described in detail in *SI Appendix, Detailed Experimental Procedures*. Computational analyses of RNA-seq data were performed as described in detail in *SI Appendix*.

Immunoblotting and protein quantifications were performed as described previously (30, 62).

Experiments Involving Mice. All mouse work was performed under approved protocols at Stanford University. Nrxn1α/β cKO mice were described previously (26). ES cells were generated from Nrxn1α/β conditional KO mice using standard procedures and converted into neurons using the standard iN cell protocol. For details, see *SI Appendix*.

Morphological Analyses Using Immunofluorescence Microscopy. Paraformaldehyde-fixed human neurons were examined by immunofluorescence staining and confocal microscopy as described previously (29, 34). Image analyses were performed using Metamorph, Nikon, and ImageJ software. For details, see *SI Appendix*.

Electrophysiological Recordings. Electrophysiological recordings from human and mouse neurons were performed as described previously (20, 30, 72), and explained in detail in *SI Appendix*.

Data and Reagent Availability. All biomaterials and data are available to the scientific community as described in detail in *SI Appendix* as follows. 1) The three schizophrenia/*NRXN1*^{del} and three control iPS cell lines (*SI Appendix*, Table S1) are available to qualified scientists from the RUCDR for the National Institute of Mental Health Repository and Genetics (Study 183) (https://www.nimhgenetics.org). RUCDR will bank and share the four engineered cKO subclones (*SI Appendix*, Table S2) when COVID-19–related laboratory restrictions have been lifted. 2) The National Cooperative Reprogrammed Cell Research Groups Cell Reprogramming Database (CReD) portal (https://cred-portal.com/) will provide open access to dendritic morphometric and synaptic density measurements, protein quantification and qRT-PCR data, electrophysiological tracings, measurements and analyses, PCR validation of the engineered iPS cell line, electrophysiological and morphometric replication data for pairs 1 and 2 (Z.P.P. laboratory), and the FCDI protocol for industrial-scale production of NGN2-induced neurons. 3) Submission to dbGAP (https://www.ncbi.nlm.nih.gov/gap/) for controlled-access sharing has been approved (Project #39338) for the following data: genomic DNA WGS data for the three *NRXN1*^{del} and three control individuals studied here and the additional lines noted above; and bulk RNA-seq data for all replicates of the nonengineered and engineered pairs presented here. 4) The following data are available through the National Center for Biotechnology Information Gene Expression Omnibus (NCBI GEO) (GSE168762): transcript-level human and mouse read counts; human counts per gene adjusted for TPM human reads; the quantile-polished $\log_2$(TPM+1) values used in the present analyses, for each of 15,000 final cluster analysis test set genes (which include the 12,910 patient-control DEG test set genes) for the 30 cultures studied here. 5) Supplementary data files for the present paper are provided as follows (the README sheet in each file provides more detailed information about its contents):

Dataset S1: Gene IDs and gene symbols and quantile polished $\log_2$(TPM+1) values for all 15,048 genes that are in the 15,000-gene cluster test set, the 12,190-gene patient-control test set, and/or the 12,356-gene engineered iN test set; and columns showing to which sets each gene belongs.

Dataset S2: Gene IDs and symbols; 4 limma *t* test values used to select 7,763 DEGs that defined clusters 1 to 7 (Fig. 7*B*); a column indicating the genes assigned to each cluster; and columns indicating which 12,910 genes were also in the patient-control test set and which of these were broadly defined up- or down-regulated patient-control DEGs.

Dataset S3: All limma output for patient-control DEG analysis of 12,910 genes in 9 patient vs. 9 control cultures; for separate analyses of each patient-control pair (3 patient vs. 3 control cultures for each pair); and for 12,356 genes for 3 deleted vs. 3 wild-type iN cultures generated from the conditional heterozygous knockout iPS cell line.

Dataset S4: All significant Bonferroni-corrected and 5% FDR GO term results for enrichments analysis of patient-control down-regulated DEGs.

Data Availability. The data reported in this paper have been deposited in the NCBI GEO database, https://www.ncbi.nlm.nih.gov/geo (accession no. GSE168762). All other study data are included in the article and supporting information.

ACKNOWLEDGMENTS. We thank Eugenia Jones (Fujifilm Cellular Dynamics) for input and advice and Steven E. Hyman (Broad Institute), Lorenz Studer (Sloan Kettering Institute), and Robert Edwards (University of California San Francisco) for their assistance throughout the study as members of the Scientific Advisory Board. This work is a component of the National Cooperative Reprogrammed Cell Research Groups to Study Mental Illness and was supported by National Institute of Mental Health (NIMH) Grants 5U19MH104172 (to D.F.L., M.W., and T.C.S.), MH122519 (to C.P.), and 2U24MH068457 (to the NIMH Repository); National Institute of Child Health and Human Development

Postdoctoral Fellowship F32HD078051 (to C.P.); the Katharine McCormick Advanced Postdoctoral Fellowship Fund (to C.P.); and the University of Massachusetts Amherst Faculty Startup Fund (to C.P.). V.R.M. was supported by a predoctoral fellowship from the National Institutes of Mental Health (F30MH108321); Y.A.H. received funding from an R00 grant during this work at Stanford (R00 AG054616). The NIMH Repository received funding from 2U24MH068457. The Stanford Schizophrenia Genetics Research Fund provided support from an anonymous donor. Bio-samples for this publication were obtained from NIMH Repository & Genomics Resource, a centralized national biorepository for genetic studies of psychiatric disorders (https://www.nimhgenetics.org/). These were peripheral blood mononuclear cell samples from National Institute of Mental Health Repository and Genomics Resource Study 29. Data and biomaterials generated in Study 29 were collected by the Molecular Genetics of Schizophrenia consortium, part 2 (MGS2), and funded by collaborative NIMH Grants MH59571 (to Evanston Northwestern Healthcare/Northwestern University), MH61675 (to Pablo V. Gejman, Collaboration Coordinator, PI, and Alan R. Sanders, Stanford University), MH67257 (to D.F.L., PI, Louisiana State University), MH59588 (to Nancy G. Buccola, PI, University of Queensland), MH59565 (to Bryan J. Mowry, PI, University of Colorado), MH59587 (to Robert Freedman, PI, and Ann Olincy, Emory University School of Medicine), MH59566 (to Farooq Amin, PI, University of Iowa), MH59586 (to Donald W. Black, PI, and Raymond R. Crowe, Mount Sinai School of Medicine), MH60870 (to Jeremy M. Silverman, PI, University of California San Francisco), MH60879 (to William F. Byerley, PI, Washington University in St. Louis), and C. Robert Cloninger (PI).

1. J. Sebat *et al*., Large-scale copy number polymorphism in the human genome. *Science* **305**, 525–528 (2004).
2. J. Sebat *et al*., Strong association of de novo copy number mutations with autism. *Science* **316**, 445–449 (2007).
3. G. Kirov *et al*., The penetrance of copy number variations for schizophrenia and developmental delay. *Biol. Psychiatry* **75**, 378–385 (2014).
4. L. Coelewij, D. Curtis, Mini-review: Update on the genetics of schizophrenia. *Ann. Hum. Genet.* **82**, 239–243 (2018).
5. D. Malhotra, J. Sebat, CNVs: Harbingers of a rare variant revolution in psychiatric genetics. *Cell* **148**, 1223–1241 (2012).
6. K. Ahn *et al*., High rate of disease-related copy number variations in childhood onset schizophrenia. *Mol. Psychiatry* **19**, 568–572 (2014).
7. C. R. Marshall *et al*.; Psychosis Endophenotypes International Consortium; CNV and Schizophrenia Working Groups of the Psychiatric Genomics Consortium, Contribution of copy number variants to schizophrenia from a genome-wide study of 41,321 subjects. *Nat. Genet.* **49**, 27–35 (2017).
8. E. Rees *et al*., Analysis of copy number variations at 15 schizophrenia-associated loci. *Br. J. Psychiatry* **204**, 108–114 (2014).
9. G. Kirov, CNVs in neuropsychiatric disorders. *Hum. Mol. Genet.* **24**, R45–R49 (2015).
10. Z. Hu, X. Xiao, Z. Zhang, M. Li, Genetic insights and neurobiological implications from NRXN1 in neuropsychiatric disorders. *Mol. Psychiatry* **24**, 1400–1414 (2019).
11. E. Kasem, T. Kurihara, K. Tabuchi, Neurexins and neuropsychiatric disorders. *Neurosci. Res.* **127**, 53–60 (2018).
12. T. C. Südhof, Synaptic neurexin complexes: A molecular code for the logic of neural circuits. *Cell* **171**, 745–769 (2017).
13. C. Lowther *et al*., Molecular characterization of NRXN1 deletions from 19,263 clinical microarray cases identifies exons important for neurodevelopmental disease expression. *Genet. Med.* **19**, 53–61 (2017).
14. P. Castronovo *et al*., Phenotypic spectrum of NRXN1 mono- and bi-allelic deficiency: A systematic review. *Clin. Genet.* **97**, 125–137 (2020).
15. Schizophrenia Working Group of the Psychiatric Genomics Consortium, Biological insights from 108 schizophrenia-associated genetic loci. *Nature* **511**, 421–427 (2014).
16. A. F. Pardiñas *et al*.; GERAD1 Consortium; CRESTAR Consortium, Common schizophrenia alleles are enriched in mutation-intolerant genes and in regions under strong background selection. *Nat. Genet.* **50**, 381–389 (2018).
17. M. Fromer *et al*., De novo mutations in schizophrenia implicate synaptic networks. *Nature* **506**, 179–184 (2014).
18. M. Fromer *et al*., Gene expression elucidates functional impact of polygenic risk for schizophrenia. *Nat. Neurosci.* **19**, 1442–1453 (2016).
19. S. Ripke, S. Group, M. O'Donovan, Current status of schizophrenia GWAS. *Eur. Neuropsychopharmacol.* **27**, S415 (2017).
20. P. F. Sullivan, D. H. Geschwind, Defining the genetic, genomic, cellular, and diagnostic architectures of psychiatric disorders. *Cell* **177**, 162–183 (2019).
21. L. S. Hall *et al*., A transcriptome-wide association study implicates specific pre- and post-synaptic abnormalities in schizophrenia. *Hum. Mol. Genet.* **29**, 159–167 (2020).
22. M. Missler *et al*., Alpha-neurexins couple Ca2+ channels to synaptic vesicle exocytosis. *Nature* **423**, 939–948 (2003).
23. J. Aoto, D. C. Martinelli, R. C. Malenka, K. Tabuchi, T. C. Südhof, Presynaptic neurexin-3 alternative splicing trans-synaptically controls postsynaptic AMPA receptor trafficking. *Cell* **154**, 75–88 (2013).
24. J. Aoto, C. Földy, S. M. C. Ilcus, K. Tabuchi, T. C. Südhof, Distinct circuit-dependent functions of presynaptic neurexin-3 at GABAergic and glutamatergic synapses. *Nat. Neurosci.* **18**, 997–1007 (2015).
25. G. R. Anderson *et al*., β-Neurexins control neural circuits by regulating synaptic endocannabinoid signaling. *Cell* **162**, 593–606 (2015).
26. L. Y. Chen, M. Jiang, B. Zhang, O. Gokce, T. C. Südhof, Conditional deletion of all neurexins defines diversity of essential synaptic organizer functions for neurexins. *Neuron* **94**, 611–625.e4 (2017).
27. J. Dai, J. Aoto, T. C. Südhof, Alternative splicing of presynaptic neurexins differentially controls postsynaptic NMDA and AMPA receptor responses. *Neuron* **102**, 993–1008.e5 (2019).
28. F. Luo, A. Sclip, M. Jiang, T. C. Südhof, Neurexins cluster Ca^{2+} channels within the presynaptic active zone. *EMBO J.* **39**, e103208 (2020).
29. C. Pak *et al*., Human neuropsychiatric disease modeling using conditional deletion reveals synaptic transmission defects caused by heterozygous mutations in NRXN1. *Cell Stem Cell* **17**, 316–328 (2015).
30. Y. Zhang *et al*., Rapid single-step induction of functional neurons from human pluripotent stem cells. *Neuron* **78**, 785–798 (2013).
31. S. E. Hyman, Enlisting hESCs to interrogate genetic variants associated with neuropsychiatric disorders. *Cell Stem Cell* **17**, 253–254 (2015).
32. D. M. Panchision, Concise review: Progress and challenges in using human stem cells for biological and therapeutics discovery: Neuropsychiatric disorders. *Stem Cells* **34**, 523–536 (2016).
33. J. Shi *et al*., Common variants on chromosome 6p22.1 are associated with schizophrenia. *Nature* **460**, 753–757 (2009).
34. F. Yi *et al*., Autism-associated SHANK3 haploinsufficiency causes Ih channelopathy in human neurons. *Science* **352**, aaf2669 (2016).
35. C. Pak *et al*., Rapid generation of functional and homogeneous excitatory human forebrain neurons using Neurogenin-2 (Ngn2). *Protocol Exchange* [Preprint] (2018). https://protocolexchange.researchsquare.com/article/nprot-6901/v1 (Accessed 7 May 2021).
36. J. A. Fantuzzo *et al*., *Intellicount*: High-throughput quantification of fluorescent synaptic protein puncta by machine learning. *eNeuro* **4**, ENEURO.0219-17.2017 (2017).
37. S. Hefft, U. Kraushaar, J. R. P. Geiger, P. Jonas, Presynaptic short-term depression is maintained during regulation of transmitter release at a GABAergic synapse in rat hippocampus. *J. Physiol.* **539**, 201–208 (2002).
38. L. F. Abbott, W. G. Regehr, Synaptic computation. *Nature* **431**, 796–803 (2004).
39. E. Neher, N. Brose, Dynamically primed synaptic vesicle states: Key to understand synaptic short-term plasticity. *Neuron* **100**, 1283–1291 (2018).
40. Y. Liu *et al*., Mutation analysis of the NRXN1 gene in a Chinese autism cohort. *J. Psychiatr. Res.* **46**, 630–634 (2012).
41. A. Y. Huang *et al*.; Tourette Syndrome Association International Consortium for Genetics (TSAICG); Gilles de la Tourette Syndrome GWAS Replication Initiative (GGRI), Rare copy number variants in NRXN1 and CNTN6 increase risk for Tourette syndrome. *Neuron* **94**, 1101–1111.e7 (2017).
42. A. Nag *et al*.; Tourette Syndrome Association International Consortium for Genetics, CNV analysis in Tourette syndrome implicates large genomic rearrangements in COL8A1 and NRXN1. *PLoS One* **8**, e59061 (2013).
43. P. Szatmari *et al*.; Autism Genome Project Consortium, Mapping autism risk loci using genetic linkage and chromosomal rearrangements. *Nat. Genet.* **39**, 319–328 (2007).
44. A. Guilmatre *et al*., Recurrent rearrangements in synaptic and neurodevelopmental genes and shared biologic pathways in schizophrenia, autism, and mental retardation. *Arch. Gen. Psychiatry* **66**, 947–956 (2009).
45. M. S. L. Ching *et al*.; Children's Hospital Boston Genotype Phenotype Study Group, Deletions of NRXN1 (neurexin-1) predispose to a wide spectrum of developmental disorders. *Am. J. Med. Genet. B. Neuropsychiatr. Genet.* **153B**, 937–947 (2010).
46. J. H. Trotter *et al*., Synaptic neurexin-1 assembles into dynamically regulated active zone nanoclusters. *J. Cell Biol.* **218**, 2677–2698 (2019).
47. Y. Hata, S. Butz, T. C. Südhof, CASK: A novel dlg/PSD95 homolog with an N-terminal calmodulin-dependent protein kinase domain identified by interaction with neurexins. *J. Neurosci.* **16**, 2488–2494 (1996).
48. Z. Wei *et al*., Liprin-mediated large signaling complex organization revealed by the liprin-α/CASK and liprin-α/liprin-β complex structures. *Mol. Cell* **43**, 586–598 (2011).
49. K. Tabuchi, T. Biederer, S. Butz, T. C. Sudhof, CASK participates in alternative tripartite complexes in which Mint 1 competes for binding with caskin 1, a novel CASK-binding protein. *J. Neurosci.* **22**, 4264–4273 (2002).
50. S. Butz, M. Okamoto, T. C. Südhof, A tripartite protein complex with the potential to couple synaptic vesicle exocytosis to cell adhesion in brain. *Cell* **94**, 773–782 (1998).
51. A. R. Cohen *et al*., Human CASK/LIN-2 binds syndecan-2 and protein 4.1 and localizes to the basolateral membrane of epithelial cells. *J. Cell Biol.* **142**, 129–138 (1998).Corrected in: *J. Cell Biol.* **142**, 1156 (1998).
52. Y. P. Hsueh *et al*., Direct interaction of CASK/LIN-2 and syndecan heparan sulfate proteoglycan and their overlapping distribution in neuronal synapses. *J. Cell Biol.* **142**, 139–151 (1998).
53. J. Najm *et al*., Mutations of CASK cause an X-linked brain malformation phenotype with microcephaly and hypoplasia of the brainstem and cerebellum. *Nat. Genet.* **40**, 1065–1067 (2008).
54. G. Piluso *et al*., Genetic heterogeneity of FG syndrome: A fourth locus (FGS4) maps to Xp11.4-p11.3 in an Italian family. *Hum. Genet.* **112**, 124–130 (2003).
55. H. Saitsu *et al*., CASK aberrations in male patients with Ohtahara syndrome and cerebellar hypoplasia. *Epilepsia* **53**, 1441–1449 (2012).
56. S. J. Sanders *et al*., De novo mutations revealed by whole-exome sequencing are strongly associated with autism. *Nature* **485**, 237–241 (2012).
57. B. M. Neale *et al*., Patterns and rates of exonic de novo mutations in autism spectrum disorders. *Nature* **485**, 242–245 (2012).
58. A. Hackett *et al*., CASK mutations are frequent in males and cause X-linked nystagmus and variable XLMR phenotypes. *Eur. J. Hum. Genet.* **18**, 544–552 (2010).
59. N. L. Bray, H. Pimentel, P. Melsted, L. Pachter, Near-optimal probabilistic RNA-seq quantification. *Nat. Biotechnol.* **34**, 525–527 (2016).

60. J. Zyprych-Walczak *et al*., The impact of normalization methods on RNA-seq data analysis. *BioMed Res. Int.* **2015**, 621690 (2015).
61. T. Vierbuchen *et al*., Direct conversion of fibroblasts to functional neurons by defined factors. *Nature* **463**, 1035–1041 (2010).
62. Z. P. Pang *et al*., Induction of human neuronal cells by defined transcription factors. *Nature* **476**, 220–223 (2011).
63. O. L. Wapinski *et al*., Hierarchical mechanisms for direct reprogramming of fibroblasts to neurons. *Cell* **155**, 621–635 (2013).
64. F. Kagitani *et al*., Peg5/Neuronatin is an imprinted gene located on sub-distal chromosome 2 in the mouse. *Nucleic Acids Res.* **25**, 3428–3432 (1997).
65. H. K. Evans, J. R. Weidman, D. O. Cowley, R. L. Jirtle, Comparative phylogenetic analysis of blcap/nnat reveals eutherian-specific imprinted gene. *Mol. Biol. Evol.* **22**, 1740–1748 (2005).
66. S. M. Purcell *et al*., A polygenic burden of rare disruptive mutations in schizophrenia. *Nature* **506**, 185–190 (2014).
67. T. Singh, B. M. Neale, M. J. Daly, Exome sequencing identifies rare coding variants in 10 genes which confer substantial risk for schizophrenia. *medRxiv* [Preprint] (2020). https://doi.org/10.1101/2020.09.18.20192815 (Accessed 7 May 2021).
68. R. M. Joseph, Neuronatin gene: Imprinted and misfolded: Studies in Lafora disease, diabetes and cancer may implicate NNAT-aggregates as a common downstream participant in neuronal loss. *Genomics* **103**, 183–188 (2014).
69. P. M. Pitale, W. Howse, M. Gorbatyuk, Neuronatin protein in health and disease. *J. Cell. Physiol.* **232**, 477–481 (2017).
70. S. Erhardt, L. Schwieler, L. Nilsson, K. Linderholm, G. Engberg, The kynurenic acid hypothesis of schizophrenia. *Physiol. Behav.* **92**, 203–209 (2007).
71. K. Nakazawa, K. Sapkota, The origin of NMDA receptor hypofunction in schizophrenia. *Pharmacol. Ther.* **205**, 107426 (2020).
72. A. Maximov, Z. P. Pang, D. G. R. Tervo, T. C. Südhof, Monitoring synaptic transmission in primary neuronal cultures using local extracellular stimulation. *J. Neurosci. Methods* **161**, 75–87 (2007).